Les Cahiers du GERAD ISSN: 0711–2440

Comparison of mixed integer linear models for fuel-optimal air conflict resolution with recovery

J. Omer

G–2014–41

June 2014

GERAD HEC Montréal
3000, chemin de la Côte-Sainte-Catherine
Montréal (Québec) Canada H3T 2A7

Tél. : 514 340-6053
Téléc. : 514 340-5665
info@gerad.ca
www.gerad.ca

Comparison of mixed integer linear models for fuel-optimal air conflict resolution with recovery

Jérémy Omer

GERAD & Polytechnique Montréal, Montréal (Québec) Canada, H3C 3A7

jeremy.omer@gerad.ca

June 2014

Les Cahiers du GERAD

G–2014–41

Abstract: Any significant increase in current levels of air traffic will need the support of efficient decision-aid tools. One of the tasks of air traffic management is to modify trajectories when necessary to maintain a sufficient separation between pairs of aircraft. Several algorithms have been developed to solve this problem, but the underlying assumptions are different, which makes it difficult to compare their performance. In this article, separation is maintained through changes of heading and velocity while minimizing a combination of fuel consumption and delay. For realistic trajectories, the speed is continuous with respect to time, the acceleration and turning rate are bounded, and the planned trajectories are recovered after the maneuvers. After describing the major modifications to existing models that are necessary to comply with this advanced definition of the problem, we compare three mixed integer linear programs. The first model is based on a discretization of the air space, and the second relies on a discretization of the time horizon. The third model implements a time decomposition of the problem; it allows only one initial maneuver, and it is solved periodically with a receding horizon to build a complete trajectory. The computational tests are conducted on a benchmark of artificial instances specifically built to include complex situations. Our analysis of the results highlights the strengths and limits of each model, and the time decomposition proves to be an excellent compromise.

Key Words: Air traffic control, Conflict resolution, Mixed integer linear programming.

Acknowledgments: The research presented in this article was funded by ONERA, the French Aerospace Lab, Toulouse, France.

1 Introduction

The airspace is a crowded environment requiring constant attention for both security and economic reasons. Air traffic management (ATM) is organized into successive layers corresponding to levels of anticipation that converge toward real-time. The last layer is air traffic control (ATC); for portions of the airspace outside the direct vicinity of airports, it involves monitoring traffic, establishing communication with pilots, and taking actions to ensure the fluidity and security of the traffic.

ICAO [1] translates the general concept of security into quantified criteria by defining reference distances of separation that depend on the portion of the airspace under consideration. Two aircraft are considered separated if they respect either a minimum horizontal or a minimum vertical distance, the alternative being a *loss of separation*. A *conflict* occurs when the predicted trajectories of two aircraft lead to a loss of separation. The ATC operator must detect conflicts, determine maneuvers that lead to conflict-free trajectories, and send the corresponding instructions to pilots.

Because of the potential benefits for overall ATM and the intrinsic mathematical difficulties of conflict detection and resolution (CD&R), the problem has been the focus of a large literature. The motivation is that the inclusion of an efficient and effective automated CD&R in the toolbox available to controllers could lead to a major increase in airspace capacity [2].

CD&R is a particular case of motion planning for multiple mobiles with collision avoidance. An optimal trajectory connecting two given initial and final positions is determined for each aircraft under the linking constraints that no loss of separation should occur. The cost to optimize usually reflects the flight time and fuel consumption. The result is a complex continuous-time problem in which multiple optimal trajectories are determined simultaneously with additional nonconvex separation constraints. An ideal approach should rely on general assumptions, fit the nature of the problem, and be computationally efficient. All existing studies represent a compromise among these three aspects.

Optimal control methods search for a continuous-time control law optimizing a cost functional. Since the aircraft trajectories involve continuous-time positions, speeds, and accelerations, optimal control is a logical candidate for CD&R. It allows us to derive complete models (see [3–5]), but the optimal solution can be found only for simple cases with two aircraft and a constant velocity [3]. Numerical methods are necessary to solve the problem under more general hypotheses.

If the aircraft are assumed to fly at the same altitude, one approach is to limit the possible maneuvers to a finite set of heading and/or speed changes. With this constraint, Bicchi and Pallottino [4] suggest a heuristic that builds conflict-free trajectories with sequences of straight lines and circular arcs. Frese and Beyerer [6] focus on first instantaneous heading changes with constant speed and second velocity changes with constant heading to solve the problem through a tree-exploration technique. With the same maneuvers, Durandet al. [7] develop a genetic algorithm to handle complex situations.

The second and more popular approach is to formulate the problem with discrete time. For instance, Raghunathanet al. [5] sample the time interval to focus on a finite set of variables and constraints. The resulting model is a nonlinear program (NLP) with nonconvex separation constraints. The NLP may be solved numerically, but fast algorithms cannot guarantee more than a local optimum. Borrelliet al. [8] report disappointing computational results, because a good initial point is necessary to converge to a good local optimum.

To solve the problem more efficiently, the nonlinear constraints and objective function of the NLP may be approximated with linear equations involving integer variables to obtain a mixed integer linear program (MILP). MILPs have been very popular in ATC, because they may achieve a good approximation of the NLP (see [9]),and implementations of state-of-the-art algorithms (e.g., CPLEX[1] or Gurobi [10]) find optimal solutions of large instances in a reasonable time. For instance, Schouwenaars [11] and Omer and Farges [12] develop time-discretized MILPs.

[1]CPLEX is freely available for academic and research purposes under the IBM academic initiative: http://www-03.ibm.com/ibm/university/academic

An extreme time sampling is to take only the two extremities. In this case, the conflicts resolution must be achieved with one initial maneuver per aircraft, thus leading to a simpler form of the NLP. In particular, the separation constraints become a disjunction of two linear constraints. Such models appear in [13–15].

MILPs also arise from *space discretization*. Instead of sampling the time interval, these models reduce the airspace to a finite set of important points, namely the initial and final points of the trajectories and the points where pairs of trajectories intersect. Since space discretization makes it hard to represent geographic deviations from the predicted trajectories, in these models the maneuvers are usually restricted to speed changes [16–19]. However, Omer [20] develops a space-discretized model that includes heading changes.

Despite the abundant literature on CD&R, there has been little experimental comparison of different models. Frese and Beyerer [21] conduct an experimental study, but it is limited to the avoidance of collisions between cars. In [8, 12], results are presented for an NLP and an MILP, but these models do not have to be opposed. MILP may be used as a first step toward the final result by providing a starting point for the NLP [12]. The first motivation for this article is to alleviate the overwhelming feeling induced by the multitude of models. Since a large proportion of the existing models are MILPs and they represent a wide range of options, this work focuses on MILPs. Based on the literature review above, we consider three different families of MILPs: time-discretized models with potentially more than one maneuver per aircraft, time-discretized models with at most one maneuver per aircraft, and space-discretized models.

A major obstacle is that every existing model is based on specific hypotheses. The hypotheses made in the space-discretized model of Omer [20] represent the most complete description of the problem:

- fuel consumption and delays are minimized;
- speed and heading changes are allowed;
- speed and heading are continuous functions of time;
- velocity, acceleration, and turning rate are bounded;
- aircraft must revert to their planned trajectories.

For a meaningful comparison of the families of models, they must all be based on the same hypotheses. Our first major contribution is thus to modify existing time-discretized and one-maneuver models with this goal in mind. Our second major contribution is an experimental comparison of the three models. We generate a large set of benchmark instances to ensure that the conclusions illustrate general tendencies, and we highlight the main features of each family of model. The most interesting result is that the one-maneuver model emerges as an excellent compromise.

Our approach is based on the formal definition of the problem given in Section 2. In Section 3, we briefly describe a previously developed space-discretized model. Our original modeling contribution includes the insertion of fuel consumption in a time-discretized model in Section 4 and a larger revision of a one-maneuver model in Section 5. Based on experimental tests, we compare the models in Section 6.

2 Formal definition of the conflict resolution problem

The conflict resolution problem aims to keep a set $\mathcal{A}$ of aircraft separated on a time interval $[0, T]$. Given a set of pairs of aircraft in potential conflict $\mathcal{C}$, a new trajectory is planned for each aircraft $A_i \in \mathcal{A}$ so that each pair in $\mathcal{C}$ respects the reference separation distances.

2.1 Dynamics of the aircraft

The motion of an aircraft $A_i \in \mathcal{A}$ is described by its position $\boldsymbol{p}_i(t)$, speed $\boldsymbol{v}_i(t)$, and acceleration $\boldsymbol{u}_i(t)$ at each time $t \in [0, T]$. The particular problem we are focusing on deals with **planar and deterministic motion**. These two restrictive hypotheses are reasonable for short-term traffic control focusing on portions of the airspace outside the proximity of airports, where the altitude of an aircraft is constant most of the time. In this case, a typical value of T is 10 to 15 minutes, and separation needs to be achieved through

heading and speed maneuvers. $\boldsymbol{p}_i(t)$, $\boldsymbol{v}_i(t)$, and $\boldsymbol{u}_i(t)$ are thus two-dimensional vectors, and their relation is given by the simple dynamical system:

$$\begin{pmatrix} \frac{\mathrm{d}\boldsymbol{p}_i(t)}{\mathrm{d}t} \\ \frac{\mathrm{d}\boldsymbol{v}_i(t)}{\mathrm{d}t} \end{pmatrix} = \begin{pmatrix} \boldsymbol{v}_i(t) \\ \boldsymbol{u}_i(t) \end{pmatrix}. \tag{1}$$

A reasonable level of realism is ensured by assuming that **acceleration is stepwise constant**. In other words, the maneuvers are executed with a constant acceleration vector, and the speed vector remains constant between two consecutive maneuvers. This assumption is consistent with the continuity of speed with respect to time and the need to execute maneuvers smoothly.

The dynamics of an aircraft are constrained by its performance and the comfort of passengers. The performance imposes a minimum and a maximum speed, but, as specified in [22], large velocity decreases below the preferred value are usually not appreciated by pilots. As a consequence, the minimum velocity is the larger of the value based on the aircraft's performance and that based on the pilots' preferences. In addition, the comfort of the passengers requires that the velocity and heading do not change too abruptly. This leads to maximum values for the derivatives of the speed vector's norm and argument, which are called the "acceleration" and "yaw rate" in what follows. The constraints are formalized as: $\forall t \in [0, T]$,

$$V_i^{\min} \leq V_i(t) \leq V_i^{\max}, \tag{2}$$

$$\left|\frac{\mathrm{d}\chi_i(t)}{\mathrm{d}t}\right| \leq \omega_i^{\max} \quad \text{and} \quad \left|\frac{\mathrm{d}V_i(t)}{\mathrm{d}t}\right| \leq U_i^{\max}, \tag{3}$$

where $\chi_i(t)$ is the heading and V_i is the norm of the speed vector of A_i at time t.

2.2 Ensuring separation

Since the motions of the aircraft are planar, only the horizontal separation is considered. The distance between each pair of conflicting aircraft must be greater than or equal to the reference horizontal distance of separation D:

$$\left\|\boldsymbol{p}_j(t) - \boldsymbol{p}_i(t)\right\| \geq D, \forall (A_i, A_j) \in \mathcal{C}, \forall t \in [0, T], \tag{4}$$

where $\|\cdot\|$ is the Euclidean norm.

2.3 Reverting to the planned trajectory

Trajectory recovery reflects the natural idea that a conflict resolution should minimize perturbations to the overall trajectory of an aircraft. Moreover, several projects consider a trajectory-based ATM in which both the airlines and ATC commit to do all they can to keep each aircraft as close as possible to a previously negotiated *business trajectory* (BT) (see [23]).

Both space and time deviations from the BT are controlled. A constraint is added for each aircraft to recover the course of its planned trajectory:

$$\left\langle \boldsymbol{p}_i(T) - \boldsymbol{p}_i^T \,\middle|\, \boldsymbol{n}_i^T \right\rangle = 0 \; \forall A_i \in \mathcal{A}, \tag{5}$$

where $\boldsymbol{p}_i^T$ and $\boldsymbol{v}_i^T$ are the planned position and speed of A_i at time T, $\boldsymbol{n}_i^T$ is any vector orthogonal to $\boldsymbol{v}_i^T$, and $\langle . | . \rangle$ is the scalar product. The temporal aspect of trajectory recovery is taken into consideration through a penalty in the cost function rather than a hard constraint. This issue is dealt with in the next section.

2.4 Cost minimization

The economic efficiency of a flight is usually measured by the duration and the fuel consumption. Fuel-optimal conflict-free trajectories are determined, for instance, in [14], although duration is not explicitly taken into consideration. In this work, the trajectories minimize a combination of the fuel consumption of the aircraft and the time deviations from the BT at time T.

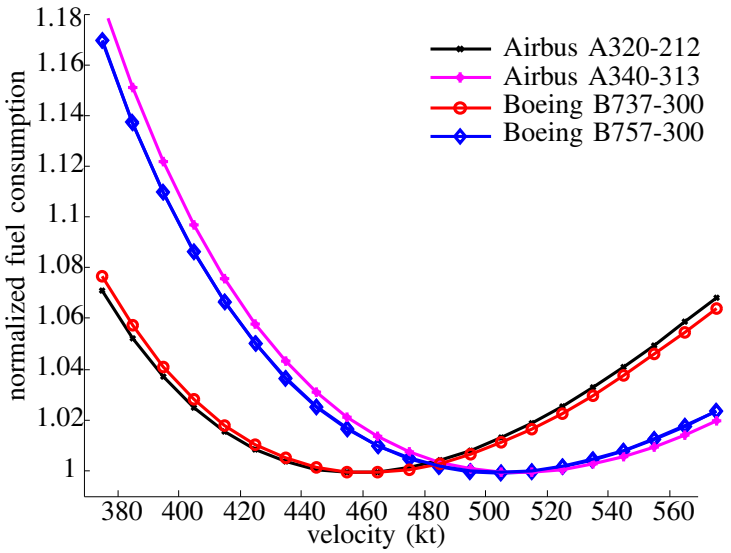

Figure 1: Fuel consumption per distance unit; the profiles are normalized by setting the minimum consumption equal to 1.0

As in [14], we use the BADA user manual [24] as the reference physical model from which the fuel consumption is derived. Sample consumption profiles are plotted in Figure 1.

Constraint (5) ensures that there is no lateral deviation from the BT at time T, so the time deviation from the BT at T is proportional to the longitudinal deviation (with a $\frac{1}{V_i^{\text{nom}}}$ factor). To penalize the time deviation, we assume that the aircraft must eventually make up the delay. Since this operation is not an emergency, the speed should not be pushed to its limit, so $\frac{1}{2}(V_i^{\text{nom}}+V_i^{\max})$ or $\frac{1}{2}(V_i^{\text{nom}}+V_i^{\min})$ are acceptable speeds, depending on the sign of the delay. Two penalties for respectively being behind or ahead of the BT, ρ_i^- and ρ_i^+, are thus computed as the additional fuel consumption needed to return to the BT. Denoting respectively $\Delta_{\parallel,i}^-$ and $\Delta_{\parallel,i}^+$ the negative and the positive longitudinal gaps from the BT at time T, it is possible to penalize these gaps with two costs ρ_i^- and ρ_i^+ respectively. A detailed description of the computation of ρ_i^- and ρ_i^+ is given in [9].

3 Space-discretized model

3.1 Principle of the space discretization

Space discretization focuses on the points of the airspace that are most likely to be important for the conflict resolution. These are the initial positions, the predicted final positions of the aircraft, and the *conflict points*, i.e., the points where the trajectories of two conflicting aircraft intersect. Although it is not identified as such, a space discretization is used in [16, 17, 19] to derive a model involving only speed maneuvers. The main contribution of a previous work [20] is to include heading maneuvers. Since we implement the same model, we describe only the principles of space discretization and the assumptions made to allow for a linear formulation with heading maneuvers. See the original description of the model for a complete mathematical formulation.

For given traffic, space discretization leads to a directed graph $(\mathcal{N}, \mathcal{E})$, where $\mathcal{N}$ is the union of the following set of nodes:

- $\mathcal{N}_I$: nodes corresponding to the initial positions;
- $\mathcal{N}_C$: nodes corresponding to the conflict points;
- $\mathcal{N}_T$: nodes corresponding to the positions at time T.

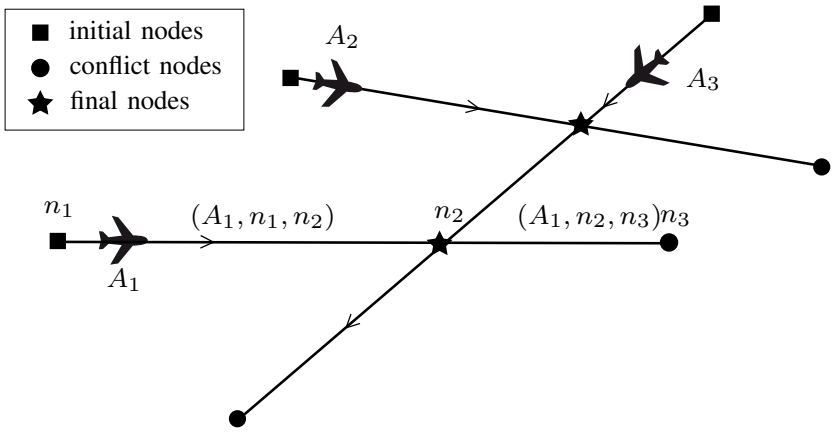

Figure 2: Conflict graph for a situation with three aircraft [20]

$\mathcal{E}$ is then built by adding, for each aircraft, the pairs of consecutive nodes over which the aircraft flies. Since a given pair of nodes (n_k, n_p) may define several edges if several aircraft fly over n_k and n_p, the edge corresponding to the BT of $A_i \in \mathcal{A}$ is denoted (A_i, n_k, n_p). Figure 2 illustrates the structure of a conflict graph for a situation involving three aircraft.

The conflict graph is completely built based on the BTs. In the model, the structure of the graph is thus fixed. The variable features of the graph are the characteristics of the edges. For instance, a speed change modifies the flight time, and heading maneuvers stretch out the length of an edge while introducing a lateral shift with respect to the BT.

In a time discretization, the separation constraints focus on the positions of two conflicting aircraft, whereas in a spatial discretization they focus on fly-over instants. Specifically, the instants that A_i and A_j fly over the conflict point must be separated with a minimum time separation $T_{i,j}^{\min}$ depending on the angle between the trajectories of the two aircraft and on their velocities. If the velocities V_i and V_j are constant and so is the angle, θ_{ij}, between the trajectories of A_i and A_j, $T_{i,j}^{\min}$ may be computed as in [16]:

$$T_{i,j}^{\min} = \frac{D}{V_i V_j \left|\sin\theta_{i,j}\right|} \sqrt{(V_i)^2 + (V_j)^2 - 2V_i V_j \cos\theta_{i,j}}.$$

The combinatorics intrinsic to the problem appears in the choice of the aircraft that passes first at the conflict point. This is modeled with two *big-M* constraints that involve one binary variable δ_{ij} and a large constant value M. The considerable strength of this model is that it involves only one binary variable per conflict. Let T_i and T_j be the fly-over times of A_i and A_j at the conflict point; then the separation constraints corresponding to the conflict are

$$T_i - T_j \geq T_{i,j}^{\min} - M\delta_{ij}, \text{ and } T_j - T_i \geq T_{i,j}^{\min} - M(1-\delta_{ij}),$$

with $\delta_{ij} \in \{0, 1\}$.

3.2 Including heading maneuvers

The maneuvers induce nonlinear modifications of the characteristics of the edges if they do not follow any specific pattern. As a consequence, the maneuvers are restricted to those corresponding to a combination of the patterns represented in Figure 3, and they cannot extend over more than one edge. In the heading maneuver depicted in Figure 3a, the aircraft has the same heading at the beginning and at the end of the maneuver: the purpose is to move the aircraft away laterally from its BT or to spatially recover it. The speed maneuvers illustrated in Figure 3b end with the same speed as they started: their purpose is to move the aircraft back or forward temporally (or longitudinally) from its BT. These maneuvers are called trapezoidal speed and heading changes in reference to the shape of the graphs of speed and heading as functions of time.

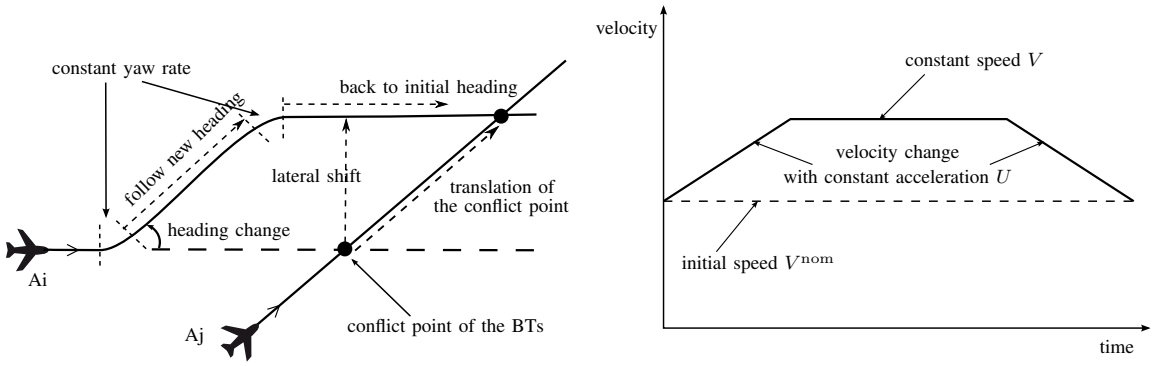

(a) Heading maneuver (b) Speed maneuver

Figure 3: Representation of the two permitted types of maneuvers

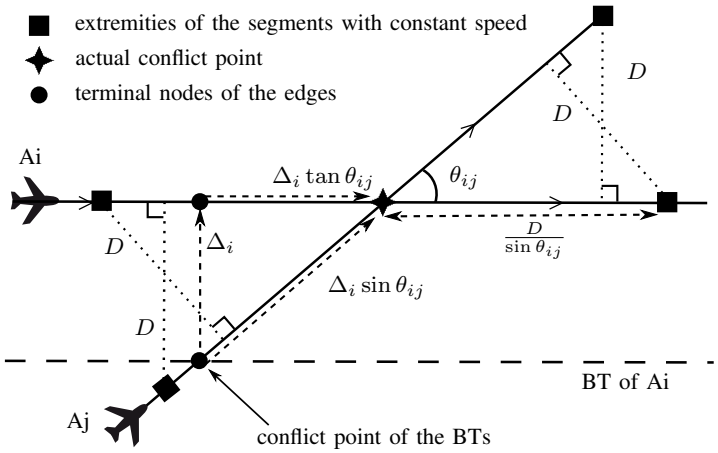

Figure 4: Focus on a crossing conflict in presence of a lateral shift

Finally, they are executed with the maximum turning rate or acceleration to minimize the transition between the initial and final speeds or headings.

The contribution of [20] relies on the fact that a trapezoidal heading change generates a lateral shift with the BT, which can in turn be converted into a temporal shift at the conflict point if the speed is constant around this point. Figure 4 illustrates that if A_i is laterally shifted by Δ_i then the conflict point is moved by a distance $\Delta_i \tan\theta_{ij}$ along the trajectory of A_i, and by a distance $\Delta_i \sin\theta_{ij}$ along the trajectory of A_j. Assuming that the velocities of A_i and A_j are constant, T_i and T_j are linear functions of the decision variables. The resulting restriction is that the speed vectors of the aircraft must be set to a constant value around the conflict points so that the separation constraints remain valid. For this, the speed vectors are constant on the segments where the distance between the trajectories is less than or equal to the reference separation distance D. As depicted in Figure 4, this corresponds to an interval of length $2\frac{D}{\sin\theta_{ij}}$ centered on the conflict point.

Finally, a stepwise linear approximation of the fuel consumption is minimized, and the recovery of the BT is ensured by demanding a zero lateral shift and minimizing the time shift at the nodes of $\mathcal{N}_T$.

The overall model is called SPACE.

4 Time-discretized model

Two operations are performed sequentially to transform the original optimal control problem into an MILP. The problem is first expressed with a finite number of variables and constraints. The nonlinear equations of the model are then approximated with linear expressions. A complete description of this process appears in [12] for a model that involves the constraints of the problem definition but a different objective. We present below a synthesis of this work that takes into account the fuel consumption.

4.1 A time-discretized model

The simplest time-discretization is done by sampling $[0, T]$ according to a constant step h. The model then focuses on a sequence of $K + 1$ times, $0 = t_0 < t_1 < \cdots < t_K = T$.

The linearization then relies on two related techniques that are most clearly understood via a geometric representation of the constraints. Separation constraints and bounds on speed and acceleration share one important characteristic: they can be seen as quadratic constraints. A convenient way to describe them involves a circle inside or outside of which the endpoint of a vector depending on the constraint must lie. Figure 5a gives a representation of the separation constraints in the mobile frame attached to one conflicting aircraft, while bounds on the velocity appear in Figure 5b. These figures also show how the circles are approximated by a set of tangents or chords to obtain a set of linear constraints ensuring that the initial quadratic constraints are satisfied.

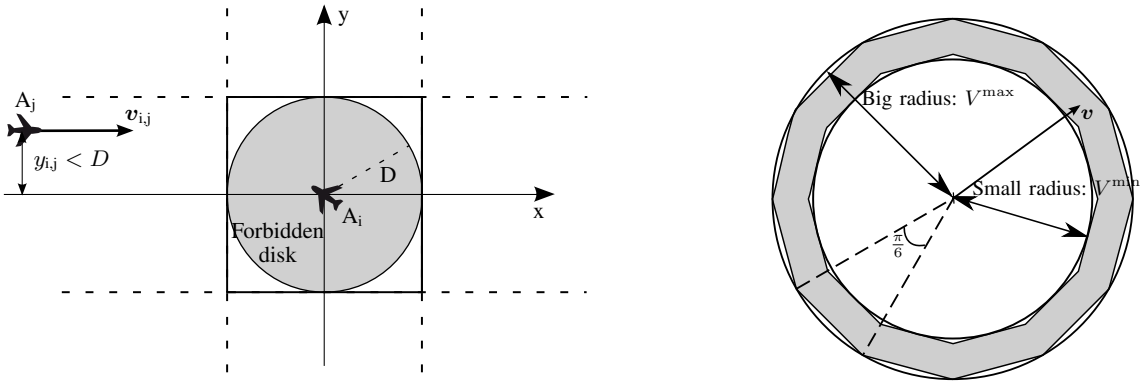

(a) Separation constraints

(b) Velocity bounds

Figure 5: Geometrical representation of separation and velocity constraints

Before focusing on the new objective function, we describe the time-discretized MILP of [12]. For convenience, we introduce the two sets $\mathcal{T} = \{t_k\}_{k=0,\dots,K}$ and $\mathcal{T}^- = \{t_k\}_{k=0,\dots,K-1}$, and the value that a function f takes at an instant $t_k \in \mathcal{T}$ is denoted $f^k = f(t_k)$. N_v and N_s are respectively the number of linear constraints used to approximate the velocity and separation constraints, $\Theta_v = \{\frac{2n\pi}{N_v}\}_{n=0,\dots,N_v-1}$, $\Theta_s = \{\frac{2n\pi}{N_s}\}_{n=0,\dots,N_s-1}$, and $\boldsymbol{e}_\theta$ is the unit vector with coordinates $(\cos\theta, \sin\theta)$.

$$\min \sum_{A_i \in \mathcal{A}} \sum_{t_k \in \mathcal{T}^-} h \cdot \overline{u}_i^k, \quad \text{subject to:} \tag{6}$$

$$\forall A_i \in \mathcal{A}:$$

$$(\boldsymbol{p}_i^0, \boldsymbol{p}_i^K) = (\boldsymbol{p}_i^{\mathrm{BT}}(0), \boldsymbol{p}_i^{\mathrm{BT}}(T)) \tag{7}$$

$$\forall A_i \in \mathcal{A},\ \forall t_k \in \mathcal{T}:$$

$$\boldsymbol{p}_i^{k+1} = \boldsymbol{p}_i^k + h \times \boldsymbol{v}_i^k + \frac{h^2}{2}\boldsymbol{u}_i^k, \tag{8}$$

$$\left\langle \boldsymbol{v}_i^k \middle| \boldsymbol{e}_\theta \right\rangle \leq \overline{v}_i^k \cos\left(\frac{\pi}{N_v}\right), \forall \theta \in \Theta_v \tag{9}$$

$$\left\langle \boldsymbol{v}_i^k \middle| \boldsymbol{e}_\theta \right\rangle \geq \underline{v}_i^k - M_v \epsilon_i^{k\theta}, \forall \theta \in \Theta_v \tag{10}$$

$$\sum_{\theta \in \Theta_v} \epsilon_i^{k\theta} = N_v - 1, \tag{11}$$

$$V_i^{\min} \leq \underline{v}_i^k \leq V_i^{\max}, V_i^{\min} \leq \overline{v}_i^k \leq V_i^{\max}, \tag{12}$$

$\forall A_i \in \mathcal{A},\ \forall t_k \in \mathcal{T}^- :$

$$\boldsymbol{v}_i^{k+1} = \boldsymbol{v}_i^k + h \times \boldsymbol{u}_i^k,\ \forall i \in \mathcal{A}, \tag{13}$$

$$\left\langle \boldsymbol{u}_i^k \middle| \boldsymbol{e}_\theta \right\rangle \leq \overline{u}_i^k \cos\left(\frac{\pi}{N_u}\right), \forall \theta \in \Theta_u, \tag{14}$$

$$\overline{v}_i^{k+1} - \underline{v}_i^k \leq h U_i^{\max}, \tag{15}$$

$$\underline{v}_i^{k+1} - \overline{v}_i^k \geq -h U_i^{\max}, \tag{16}$$

$$\overline{u}_i^k \leq \omega_i^{\max} \underline{v}_i^k, \tag{17}$$

$\forall (A_i, A_j) \in \mathcal{C}, \forall t_k \in \mathcal{T}^-, \forall \theta \in \Theta_s :$

$$\left\langle \boldsymbol{p}_j^k - \boldsymbol{p}_i^k \middle| \boldsymbol{e}_\theta \right\rangle \geq D + \frac{h^2}{8}\left(\overline{u}_i^k + \overline{u}_j^k\right) - M\delta_{ij}^{k\theta}, \tag{18}$$

$$\left\langle \boldsymbol{p}_j^{k+1} - \boldsymbol{p}_i^{k+1} \middle| \boldsymbol{e}_\theta \right\rangle \geq D + \frac{h^2}{8}\left(\overline{u}_i^k + \overline{u}_j^k\right) - M\delta_{ij}^{k\theta}, \tag{19}$$

$$\sum_{\theta \in \Theta_s} \delta_{ij}^{k\theta} = N_s - 1, \tag{20}$$

$\forall A_i \in \mathcal{A},\ \forall t_k \in \mathcal{T} :$

$\boldsymbol{p}_i^k \in \mathbb{R}^2, \boldsymbol{v}_i^k \in \mathbb{R}^2, \overline{v}_i^k \geq 0, \underline{v}_i^k \geq 0,$

$\epsilon_i^{k\theta} \in \{0,1\}, \forall \theta \in \Theta_v$

$\forall A_i \in \mathcal{A},\ \forall t_k \in \mathcal{T}^- : \boldsymbol{u}_i^k \in \mathbb{R}^2, 0 \leq \overline{u}_i^k \leq U_i^{\max}$

$\forall (A_i, A_j) \in \mathcal{C}, \forall t_k \in \mathcal{T}^-, \forall \theta \in \Theta_s : \delta_{ij}^{k\theta} \in \{0,1\}$

Constraints (8) and (13) describe the dynamics of the aircraft assuming that the acceleration vectors are constant on each subinterval $[t_k, t_k + 1], t_k \in \mathcal{T}^-$. Constraints (9)–(12) specify the upper bounds on the velocity, and (10)–(11) represent the lower bounds. The upper bounds on the acceleration and yaw rate are respectively given by (14)–(16) and (17). Separation is guaranteed by (18)–(20).

Two modeling techniques need to be explained. First, the approximation with tangents is actually a disjunction since one of the tangent constraints must be satisfied. As in SPACE, this is modeled with a set of big-M constraints involving as many binary variables as tangents. Constraints (11) and (20) then guarantee that at least one tangent constraint is satisfied.

Second, the constraints on the velocity and acceleration (9)–(10) and (14) include a set of variables $\underline{v}, \overline{v}$, and $\overline{u}$ where one would expect to find the minimum and maximum velocities and the maximum acceleration $V^{\min}$, $V^{\max}$, and $U_i^{\max}$. This gives access to lower and upper bounds on the velocity and acceleration, which may in turn be used to get linear expressions for several constraints and the objective function. For instance, the natural expression for the maximum acceleration of A_i is nonlinear: $\left|\left\|\boldsymbol{v}_i^{k+1}\right\| - \left\|\boldsymbol{v}_i^k\right\|\right| \leq U_i^{\max}$. Since (9)–(10) ensure that $\underline{v}_i^k \leq \left\|\boldsymbol{v}_i^k\right\| \leq \overline{v}_i^k$ and $\underline{v}_i^{k+1} \leq \left\|\boldsymbol{v}_i^{k+1}\right\| \leq \overline{v}_i^{k+1}$, (15)–(16) are valid linear constraints. A similar reasoning reveals that the minimized criterion is the sum of the norms of the acceleration vectors.

For more details about the quality of the constraints, the computation of efficient M values, and the addition of valid cuts to speed up the solution, see [9, 12].

4.2 Minimizing a meaningful objective function

The model given in the previous subsection minimizes acceleration and requires a complete recovery of the BTs. Our intent is to relax the time recovery and minimize a combination of fuel consumption and delay.

The fuel consumption per time unit is a nonlinear function of velocity. Two approximations lead to a linear expression. First, the velocity is approximated on each subinterval of time $[t_k, t_{k+1}]$ by the average value $\frac{1}{2}\left(\left\|\boldsymbol{v}_i^k\right\| + \left\|\boldsymbol{v}_i^{k+1}\right\|\right)$. Second, the fuel consumption is approximated with a stepwise linear function joining $N_Z + 1$ points of the real curve. This provides a very good estimation of the fuel consumption for as few as four segments, as illustrated in Figure 6 for an Airbus A320 at 33,000 feet.

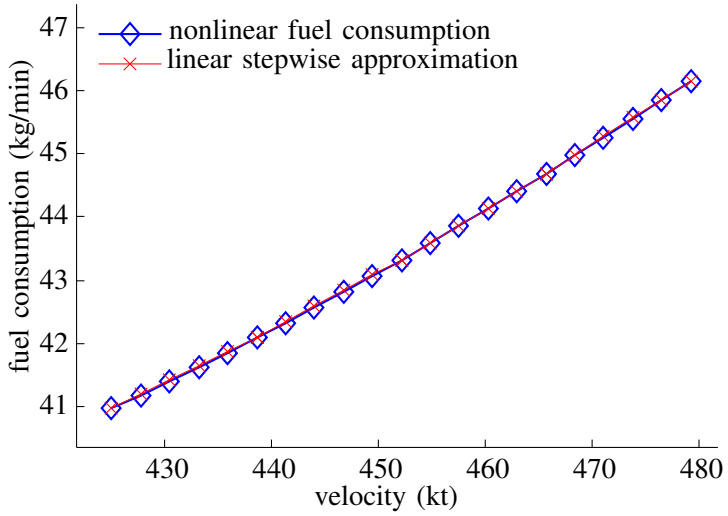

Figure 6: Fuel consumption per time unit: original function and stepwise approximation for an Airbus A320 at 33,000 feet

For a particular aircraft $A_i \in \mathcal{A}$, let $Z = \alpha_i^n V + \beta_i^n$ be the equation of the n^{th} segment, with $n \in \{1, \ldots, N_Z\}$. The fuel-consumption function was found to be convex on the interval $[V^{\min}, V^{\max}]$ for all the aircraft types that were tested. Let $\widetilde{z}_i^k$ be the approximate fuel consumption on $[t_k, t_{k+1}]$; then, for all $n \in \{1, \ldots, N_Z\}$,

$$\widetilde{z}_i^k \geq h \times \left(\frac{\alpha_n}{2}\left(\left\|\boldsymbol{v}_i^k\right\| + \left\|\boldsymbol{v}_i^{k+1}\right\|\right) + \beta_n\right). \tag{21}$$

If the value of $\widetilde{z}_i^k$ is minimized subject to the above constraint, it will exactly follow one of the N_Z segments. Now, recall that $\overline{v}_i^k \geq \left\|\boldsymbol{v}_i^k\right\|$. As a consequence, instead of (21) we add the following linear constraints to the model:

$$\widetilde{z}_i^k \geq h \times \left(\frac{\alpha_n}{2}\left(\overline{v}_i^k + \overline{v}_i^{k+1}\right) + \beta_n\right), n = 1, \ldots, N_Z. \tag{22}$$

Space recovery is then enforced by adding constraint (5), and the delay is minimized by penalizing the longitudinal deviations:

$$\sum_{A_i \in \mathcal{A}} \sum_{t_k \in \mathcal{T}^-} z_i^k + \left(\Delta_{\parallel,i}^+ + \Delta_{\parallel,i}^-\right) \times C_{d,i}\left(V_i^{\text{nom}}\right) + \rho_i^+ \Delta_{\parallel,i}^+ + \rho_i^- \Delta_{\parallel,i}^-. \tag{23}$$

The complete model, called TIME, consists in minimizing (23) subject to (8)–(20), (5), and (22).

5 The one-maneuver simplification

The specificity of this model is that it describes a conflict resolution involving only one maneuver for each aircraft, all these maneuvers being executed simultaneously at the initial time. It is similar to the model of Vela et al. [14] but it makes several improvements:

- speed changes are not assumed to be instantaneous;
- both the acceleration and yaw rate are constrained;

- the fuel-consumption equations involve continuous variables instead of the SOS2 variables that lead to a larger exploration tree;
- the space and time recovery of the BT are explicit.

Moreover, the resulting model is solved multiple times with a receding horizon to allow for the same number of maneuvers as in TIME.

5.1 Description of the simplified model

The maneuvers are assumed to be performed with a constant acceleration vector during a given time step of length h. Starting with known position and speed vectors, $\boldsymbol{p}_i^{\text{ini}}$ and $\boldsymbol{v}_i^{\text{ini}}$, the movement of an aircraft A_i is thus entirely described by the target speed vector $\boldsymbol{v}_i$ that is reached at time h.

The constraints on velocity are then similar to (9)–(12), except that upper bounds on the acceleration may be directly included because the initial speed is known. $\forall A_i \in \mathcal{A}$,

$$\langle \boldsymbol{v}_i | \, \boldsymbol{e}_\theta \rangle \leq \overline{v}_i \cos\left(\frac{\pi}{N_v}\right), \ \forall \theta \in \Theta_v \tag{24}$$

$$V_i^{\min} \leq \overline{v}_i \leq \min\left(V_i^{\max}, \left\|\boldsymbol{v}_i^{\text{ini}}\right\| + hU_i^{\max}\right), \tag{25}$$

$$\langle \boldsymbol{v}_i | \, \boldsymbol{e}_\theta \rangle \geq \max\left(V_i^{\min}, \left\|\boldsymbol{v}_i^{\text{ini}}\right\| + hU_i^{\max}\right) - M_v \epsilon_i^\theta, \ \forall \theta \in \Theta_v \tag{26}$$

$$\sum_{\theta \in \Theta_v} \epsilon_i^\theta = N_v - 1 \tag{27}$$

$$\epsilon_i^\theta \in \{0, 1\}, \ \forall \theta \in \Theta_v \tag{28}$$

The upper bound on the yaw rate is also easily expressed with linear constraints involving the upper bound on the velocity, $\overline{v}$:

$$\left\langle \boldsymbol{v}_i | \, \boldsymbol{v}_i^{\text{ini}} \right\rangle \geq \overline{v}_i \left\|\boldsymbol{v}_i^{\text{ini}}\right\| \cos\left(h\omega_i^{\max}\right), \ \forall A_i \in \mathcal{A}. \tag{29}$$

The most significant effect of performing only one maneuver is that the separation constraint becomes a disjunction between two linear constraints if the speed changes are instantaneous. Figure 7 shows a conflict in the mobile frame attached to one conflicting aircraft. Geometrically, the conflict is then solved if the relative speed vector $\boldsymbol{v}_{ij}$ is outside the forbidden cone. The remaining issue is that speed changes are assumed to be done with a constant acceleration vector.

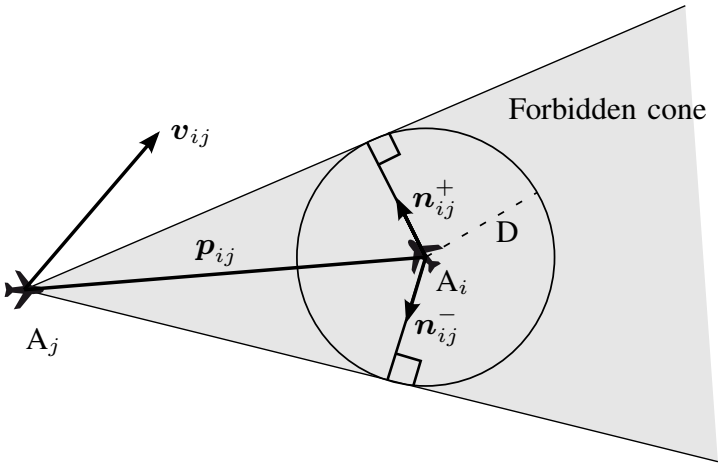

Figure 7: Conflict solved with only one instantaneous maneuver

Proposition 1 *Consider* $\boldsymbol{p}_0$, $\boldsymbol{v}_0$, $\boldsymbol{u}_0 \in \mathbb{R}^2$ *and the functions* $\boldsymbol{p}$ *and* $\widetilde{\boldsymbol{p}}$ *defined by*

$$\boldsymbol{p}(t) = \begin{cases} \boldsymbol{p}_0 + t\boldsymbol{v}_0 + \frac{t^2}{2}\boldsymbol{u}_0, 0 \le t \le h \\ \boldsymbol{p}_0 + h\boldsymbol{v}_0 + \frac{h^2}{2}\boldsymbol{u}_0 + (t-h)(\boldsymbol{v}_0 + \boldsymbol{u}_0 h), h \le t \end{cases}$$

$$\widetilde{\boldsymbol{p}}(t) = \begin{cases} \boldsymbol{p}_0 + t\boldsymbol{v}_0, 0 \le t \le \frac{h}{2} \\ \boldsymbol{p}_0 + \frac{h}{2}\boldsymbol{v}_0 + (t-\frac{h}{2})(\boldsymbol{v}_0 + \boldsymbol{u}_0 h), \frac{h}{2} \le t. \end{cases}$$

Then, $\boldsymbol{p}(t) = \widetilde{\boldsymbol{p}}(t) \forall t \ge h$.

Proposition 1 states that after a speed vector change with constant acceleration, the position is the same as if the change had been achieved instantaneously after a delay equal to $h/2$. Typically, h is set to less than one minute. Since emergencies are treated with specific protocols, no loss of separation is predicted in the time interval $[0, h]$. As a consequence, everything behaves as if speed vector changes were instantaneous and the initial positions of the aircraft were given by $\widetilde{\boldsymbol{p}}_i^{\text{ini}} = \boldsymbol{p}_i^{\text{ini}} + \frac{h}{2}\boldsymbol{v}_i^{\text{ini}}$. For a given conflict between A_i and A_j, the tangents defining the forbidden cone in Figure 7 are computed using $\widetilde{\boldsymbol{p}}_i^{\text{ini}}$ and $\widetilde{\boldsymbol{p}}_j^{\text{ini}}$ as the initial positions of the two aircraft. The two unit vectors, $\widetilde{n}_{ij}^+$ and $\widetilde{n}_{ij}^-$, orthogonal to these tangents and pointing outside the forbidden cone then give rise to the separation constraints: $\forall (A_i, A_j) \in \mathcal{C}$,

$$\left\langle \boldsymbol{v}_j - \boldsymbol{v}_i \middle| \widetilde{\boldsymbol{n}}_{i,j}^+ \right\rangle \ge -M\delta_{ij} \tag{30}$$

$$\left\langle \boldsymbol{v}_j - \boldsymbol{v}_i \middle| \widetilde{\boldsymbol{n}}_{i,j}^- \right\rangle \ge -M(1-\delta_{ij}) \tag{31}$$

$$\delta_{ij} \in \{0, 1\} \tag{32}$$

The disjunction is modeled with big-M constraints. The value of M must be such that, for any valid values of $\boldsymbol{v}_i$ and $\boldsymbol{v}_j$, (30) and (31) are respectively satisfied if $\delta_{ij} = 1$ and $\delta_{ij} = 0$. If we solve the model with a branch and bound method based on linear relaxations of the MILP, the best value of M is the smallest value that satisfies this condition, because it leads to the tightest linear relaxations. Here, we notice that

$$\left\langle \boldsymbol{v}_j - \boldsymbol{v}_i \middle| \widetilde{\boldsymbol{n}}_{i,j}^+ \right\rangle \ge -(\|\boldsymbol{v}_i\| + \|\boldsymbol{v}_j\|).$$

A good value of the constant is thus obtained by $M = V_i^{\max} + V_j^{\max}$. It is also the best value if we do not take maximum accelerations and yaw rates into account.

The estimation of the fuel consumption and delay rely on the description of a complete trajectory. It is thus necessary that the aircraft revert to their BTs. The difficulty is that an aircraft should not start a recovery maneuver while a loss of separation is possible.

Proposition 2 *Let* $(A_i, A_j) \in \mathcal{C}$ *be such that the two aircraft fly with constant speed vectors* $\boldsymbol{v}_i^{\text{ini}}$ *and* $\boldsymbol{v}_j^{\text{ini}}$. *Assume that* A_i *and* A_j *are separated at* $t = 0$ *and* $t = T$, *and that a loss of separation occurs in* $(0, T)$. *The loss of separation ends at* $t = \tau_{ij}$ *with*

$$\left\langle \boldsymbol{p}_{ij}(\tau_{ij}) \middle| \frac{\boldsymbol{v}_{ij}^{\text{ini}}}{\|\boldsymbol{v}_{ij}^{\text{ini}}\|} \right\rangle = D \Leftrightarrow \tau_{ij} = D - \left\langle \boldsymbol{p}_{ij}(0) \middle| \frac{\boldsymbol{v}_{ij}^{\text{ini}}}{\|\boldsymbol{v}_{ij}^{\text{ini}}\|} \right\rangle.$$

Proposition 2 provides an estimation of the instant when a conflict ends if no maneuver is performed. Under the same condition, an aircraft A_i will not be involved in a loss of separation after the time $\tau_i = \max\{\tau_{ij} : (A_i, A_j) \in \mathcal{C}\}$. A second virtual maneuver starting at τ_i is thus added to simulate the complete trajectory for A_i. Clearly, the estimation of the end of the conflicts is incorrect if maneuvers are performed, but it remains valid since this second maneuver is computed to estimate the fuel and delay costs. Let $\boldsymbol{v}_i'$, $A_i \in \mathcal{A}$, be the target speed vectors of this virtual recovery maneuver. Proposition 1 is applied once again to compute the final position with

$$\boldsymbol{p}_i(T) = \widetilde{\boldsymbol{p}}_i^{\text{ini}} + \tau_i \boldsymbol{v}_i + (T - \tau_i - \frac{h}{2})\boldsymbol{v}_i', \ \forall A_i \in \mathcal{A}.$$

As for TIME, the fuel consumption is approximated with a stepwise linear function, and the final position of each aircraft A_i is used to compute the longitudinal gaps $\Delta_{\parallel,i}^+$ and $\Delta_{\parallel,i}^-$. The associated constraints and objective function are then similar to (22) and (23); they are omitted to save space. The resulting MILP with one maneuver is called ONE.

5.2 Building a complete trajectory

Solving ONE produces at most one speed change for each aircraft. The second speed change that simulates the recovery of the BT is included only to estimate the overall cost of a maneuver and is not meant to lead to an actual control instruction. This recovery instruction should be sent only once all the conflicts are over, so that no loss of separation may be created by this maneuver.

For a consistent comparison with TIME, ONE is solved at each time step $t_k \in \mathcal{T}$ according to the receding-horizon procedure summarized in Algorithm 1. The result is a set of complete conflict-free trajectories reverting to the associated BTs. In Algorithm 1, the conditional loop on lines 4–7 identifies the moment when the recovery maneuver may be started. If $\tau_i \leq t_k$, then no maneuver is needed to solve the conflicts involving A_i, so it may revert to its BT. The recovery maneuver is computed to minimize a combination of the fuel consumption and the penalties due to the longitudinal deviation, as in (23).

Algorithm 1 Multiple resolution of ONE

Require: initial states $\left\{\left(\boldsymbol{p}_i^{\text{ini}}, \boldsymbol{v}_i^{\text{ini}}\right)\right\}_{A_i \in \mathcal{A}}$, final states $\{\boldsymbol{p}_i^T\}_{A_i \in \mathcal{A}}$

1: **for** $t_k \in \mathcal{T}^-$ **do**
2: **for** $A_i \in \mathcal{A}$ **do**
3: Estimate τ_i
4: **if** $\tau_i \leq t_k$ **then**
5: Compute the recovery maneuver of A_i
6: $\mathcal{A} \leftarrow \mathcal{A} \setminus A_i$
7: **end if**
8: **end for**
9: Solve ONE: the solutions are described by $\{\boldsymbol{v}_i\}_{A_i \in \mathcal{A}}$
10: **for** $A_i \in \mathcal{A}$ **do**
11: $\boldsymbol{p}_i^{\text{ini}}, \boldsymbol{p}_i^{k+1} \leftarrow \widetilde{\boldsymbol{p}}_i^{\text{ini}} + \frac{h}{2}\boldsymbol{v}_i$
12: $\boldsymbol{v}_i^{\text{ini}}, \boldsymbol{v}_i^{k+1} \leftarrow \boldsymbol{v}_i$
13: **end for**
14: **end for**

In the remainder of this article, the term ONE will refer to the model described in the previous subsection or to Algorithm 1, provided the context is unambiguous.

6 Computational experiments

6.1 Generation of a large benchmark of complex problems

The experimental comparison of TIME, ONE, and SPACE is based on the benchmark of [20], slightly extended to include larger instances. The instances implement the three global schemes depicted in Figure 8. These patterns represent complex situations in which a large number of losses of separation are predicted to occur in the next five to ten minutes. As the number of aircraft grows, the corresponding situation becomes much more complex than the most difficult situations that a controller ever deals with. The purpose of building this benchmark is thus to test the algorithms with a diverse set of conflicts and to explore their limits.

For each pattern, five to six scenarios are used to randomly generate 100 instances. The scenarios mostly differ in the number of aircraft involved. They are thus denoted by the first letter of the corresponding pattern and the number of aircraft. When we generate the instances randomly, the initial separation between aircraft flying on the same trail is set to $8 + U([-2.5, 2.5])$ NM, where $U([a, b])$ follows a uniform random law on the interval $[a, b]$. The distance between the first aircraft of each trail and the closest conflict point is also perturbed with a uniform term $U([-2.5, 2.5])$ NM, and the crossing angle α follows $U([\frac{\pi}{4}, \frac{3\pi}{4}])$ for the trail scenarios.

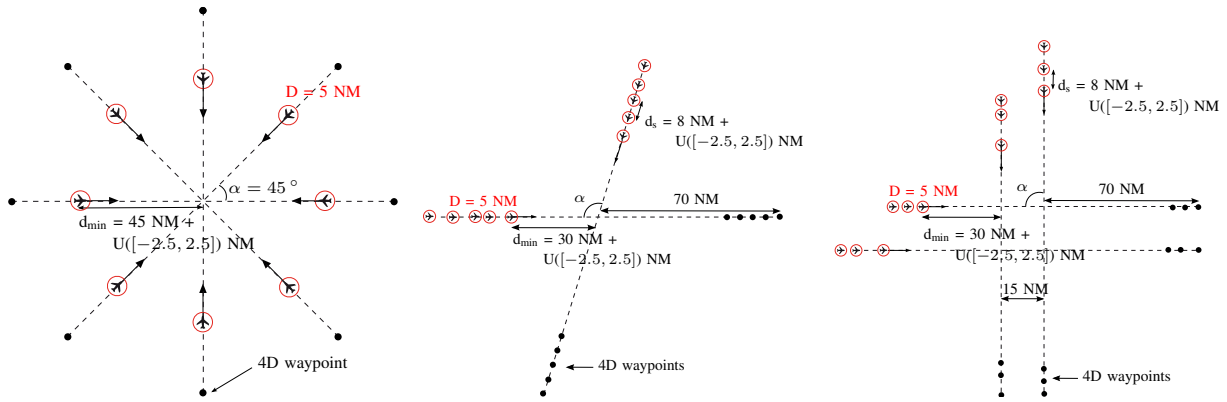

(a) Roundabout scenario (b) Trail crossing scenario (c) Grid scenario

Figure 8: Scenarios used to build the benchmark

The values of the parameters of the models are listed in Table 1. They reflect the content of BADA [24] for an Airbus A320 flying at 33,000 feet. They also ensure the comfort of passengers, according to the study of Paielli [22]. Additionally, the characteristic values of the linear approximations are set to $N_Z = 4$, $N_s = 4$, and $N_v = 36$.

Table 1: Optimization and aircraft-performance parameters

D	h	V^{nom}	V^{min}	V^{max}	U^{max}	ω^{max}
5 NM	30 s	452 kt	425 kt	479 kt	0.4 kt.s^{-1}	0.88°.s^{-1}

6.2 Analysis of the results

We solve TIME, ONE, and SPACE on 1600 instances generated randomly according to sixteen scenarios. Gurobi [10] is used with its default options to solve each MILP on a quad-core 2.5-GHz Intel processor with 4 Go of RAM. The time limit of Gurobi is set to 120 s, and we keep the best available solution when Gurobi reaches this limit. The simulation results are summarized in Figure 9. For each scenario, Figure 9a gives the number of instances for which a conflict-free solution is found, and Figures 9b and 9c give the average costs and the Gurobi runtimes respectively. The average costs are given in kilograms of fuel since the delay penalties convert the time deviations into fuel consumptions. Moreover, they take into account only the conflict-free solutions, because the costs of infeasible solutions may be exceptionally high. The scenarios are ordered on the x-axis according to the growing cost of the solutions of TIME, which is a valid measure of complexity.

Although significant differences exist between the three models, we draw the attention of the reader to the overall efficiency of the three algorithms. If we omit G12, R07, and R08, which are included primarily to test the limits of the models, a conflict-free solution is found for all the instances, and the average cost of the associated maneuvers does not exceed 10 kg per aircraft. Moreover, the computational time is always reasonable and is not far from being compatible with an operational implementation.

When we compare the curves, a gross ordering appears, with only minor exceptions if we consider G12, R07, or R08. Let $|\mathcal{S}|_{\text{MOD}}$, Z_{MOD}, and cpu_{MOD} be respectively the number of conflict-free solutions, the average cost, and the average computational time when solving MOD. Global relations exist between the three models:

$$|\mathcal{S}|_{\text{SPACE}} \leq |\mathcal{S}|_{\text{TIME}} \leq |\mathcal{S}|_{\text{ONE}} \tag{33}$$

$$\text{Z}_{\text{SPACE}} \geq \text{Z}_{\text{TIME}} \geq \text{Z}_{\text{ONE}} \tag{34}$$

$$\text{cpu}_{\text{TIME}} \geq \text{cpu}_{\text{ONE}} \geq \text{cpu}_{\text{SPACE}}. \tag{35}$$

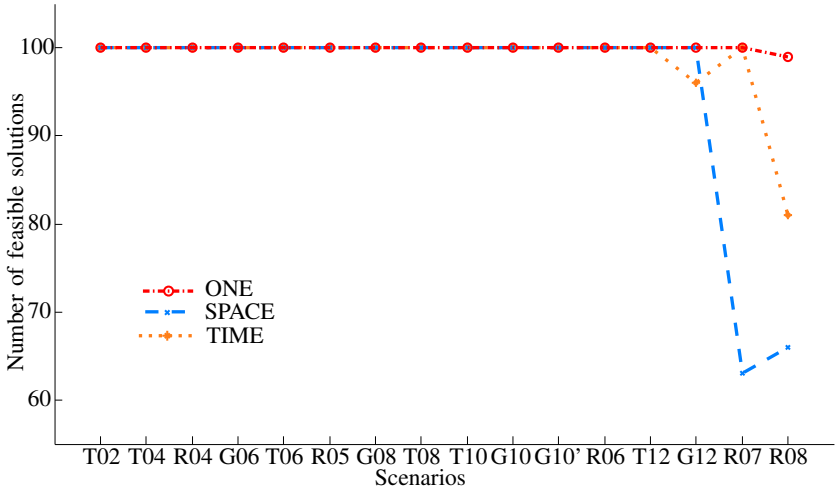

(a) Number of feasible solutions

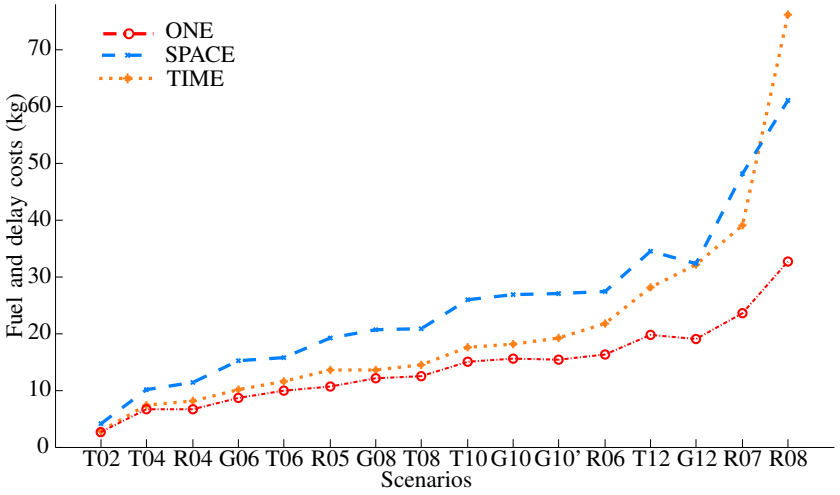

(b) Average cost of feasible solutions

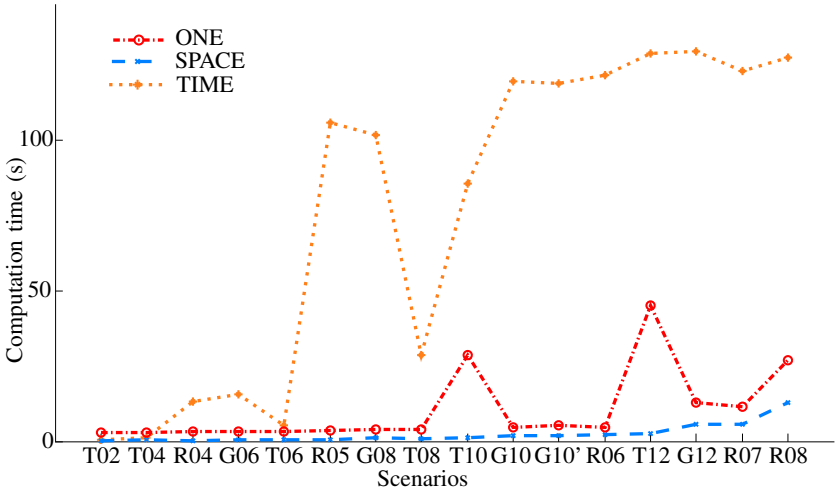

(c) Average computation time

Figure 9: Comparison of the three mixed integer linear models

The most surprising consequence of this ordering is that ONE is better than TIME on all three aspects, although ONE is presented as a simplification of TIME. The reason for this is that, although a much stronger initial hypothesis is made to build ONE, namely the limitation to one maneuver, overall it makes fewer approximations than TIME makes in the course of modeling the problem. For instance, no approximation is needed to model the separation constraints or the upper bounds on the acceleration and yaw rate. The disadvantage of ONE is the time decomposition needed to get trajectories with more than one modification of the speed vector. Since the complete solution is the aggregation of the solutions obtained at each time step, there is a necessary loss with regards to optimality. This is compensated for by the fact that maneuvers have to be started as soon as conflicts are detected to be efficient. Consequently, the maneuvers computed at the first time step need only a few adjustments during the following iterations. In terms of the computational time, ONE needs to be solved multiple times, but each call to Gurobi takes a negligible portion of the runtime needed for TIME.

In the ordering above, the model SPACE is either the worst or the best on each aspect. On the one hand, the average cost for SPACE is approximately twice that for ONE, and more than 35% of the instances of R07 and R08 had no conflict-free solutions with SPACE, while ONE fails just once. This mostly results from the need for constant speed vectors around the conflict points in SPACE; this interval encroaches upon the space available for the maneuvers. Since the size of the intervals grows with the complexity of the scenarios, there is finally insufficient space to avoid every loss of separation in R07 and R08. To a lesser extent, restricting the maneuvers of SPACE to two fixed patterns also reduces the space of the conflict-free solutions. On the other hand, SPACE is solved in a few seconds whatever the scenario. This alone could lead to a preference for SPACE over TIME, because ATC has a strong need for reactivity. ONE appears however to be a better compromise on the three aspects that we focused on. Indeed, the only advantage of SPACE is that it is solved faster than ONE, but the latter model is still solved in a small computational time. Moreover, if need be, Algorithm1 may be stopped as soon as it finds a set of speed vectors that allows us to avoid every loss of separation. In most cases, this is the first time step.

From a modeling point of view, SPACE involves tedious mathematical developments and several restrictions on the maneuvers (see [20]). This could mean that the limits of space discretization are not far from being reached, and it is hard to say whether new operational needs could be taken into account in the model without other costly approximations. In contrast, ONE is relatively simple and should allow for additional features such as uncertainties in the speed or prohibited airspace volumes.

To illustrate the qualitative behavior of the three models, Figure 10 shows the solutions they find for a roundabout instance with six aircraft. The green squares and red disks are respectively the initial and final positions in the BT. The red circles around the aircraft have a radius of 2.5 NM; they are drawn to emphasize the complexity of the situation. The figure first shows that these complex conflicts can be resolved with relatively small maneuvers giving rise to trajectories with realistic aspects. Moreover, the six aircraft revert to their BTs in the three solutions. The most obvious difference between the solutions is the trapezoidal heading maneuver pattern on the trajectories found with SPACE. The SPACE solution also exhibits larger deviations from the BT than do the other two solutions.

7 Conclusion

This article is motivated by the difficulty of objectively comparing the models and algorithms developed for the air conflict resolution problem. We focus on three mixed integer linear formulations representing the diversity of the state of the art. They are respectively obtained by focusing on a small set of points including those where trajectories intersect (SPACE), by sampling the time horizon (TIME), and by assuming that each aircraft performs only one maneuver (ONE). Based on a realistic formulation of the problem, we describe major revisions of two existing time-discretized and one-maneuver models. Every model minimizes a combination of fuel consumption and flight time and avoids losses of separation through speed and heading maneuvers. Furthermore, each aircraft respects dynamical constraints on the velocity, acceleration, and yaw rate, and each reverts to its planned trajectory after the maneuvers.

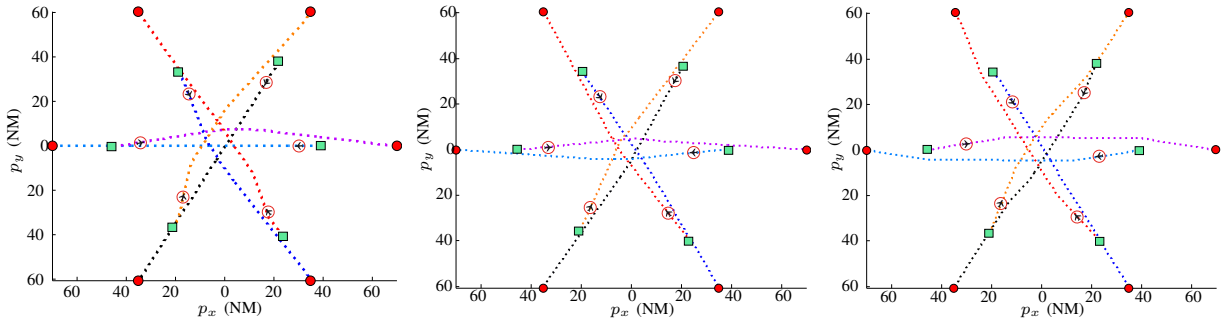

(a) Solution of TIME (b) Solution of ONE (c) Solution of SPACE

Figure 10: Solutions of an R06 instance

We then conduct a computational comparison on a benchmark of artificial instances including very complex situations. The results reveal that every model may be solved to find conflict-free and economically efficient trajectories in nearly every situation. The exceptions are scenarios that were intentionally added to test the limits of the models: they could not be handled by SPACE. Our analysis focuses on the number of conflict-free solutions, their average costs, and the computational times. It shows that the apparently simple model, ONE, represents the best compromise. The model fails to produce a conflict-free solution on only one of 16000 instances, and the computational time is compatible with an operational implementation.

Future research could carry on the computational comparison that has been started here. The most promising models and algorithms using nonlinear programming, metaheuristics, potential techniques, etc. would need to be adapted to comply with the same problem definition. A more complete comparison would also involve an extended benchmark including instances originating from real traffic data. Finally, since ONE seems simple enough to be adaptive, it would be interesting to add features that would be needed in an operational implementation. These include uncertainties in the speed, forbidden airspace volumes, conflicts involving aircraft with changing altitudes, and equity management.

References

[1] ICAO, Procedures for air navigation services – Rules for the air and traffic services, Tech. Rep., 1996.

[2] T. Lehouillier, C. Allignol, J. Omer, and F. Soumis, Interactions between operations and planning in air traffic control, in International Conference on Research in Air Transportation (ICRAT), 2014.

[3] N. Durand, Optimisation de trajectoires pour la résolution de conflits en route. Ph.D. dissertation, INPT, 1996.

[4] A. Bicchi and L. Pallottino, On optimal cooperative conflict resolution for air traffic management systems, IEEE Transactions on Intelligent Transportation Systems, 1(4), 221–231, 2000.

[5] A. U. Raghunathan, V. Gopal, D. Subramanian, L. T. Biegler, and T. Samad, Dynamic optimization strategies for three-dimensional conflict resolution of multiple aircraft, Journal of Guidance, Control, and Dynamics, 27(4), 586–594, 2004.

[6] C. Frese and J. Beyerer, Planning cooperative motions of cognitive automobiles using tree search algorithms, in KI 2010: Advances in Artificial Intelligence, ser. Lecture Notes in Computer Science, R. Dillmann, J. Beyerer, U. Hanebeck, and T. Schultz, Eds. Springer Berlin/Heidelberg, 2010, vol. 6359, pp. 91–98.

[7] N. Durand, J.-M. Alliot, and J. Noailles, Automatic aircraft conflict resolution using genetic algorithms, in Symposium on Applied Computing, 1996.

[8] F. Borrelli, D. Subramanian, A. U. Raghunathan, and L. T. Biegler, MILP and NLP techniques for centralized trajectory planning of multiple unmanned air vehicles, in American Control Conference, vol. 1–12, 2006, Proceedings Paper, pp. 5763–5768.

[9] J. Omer, Modèles déterministes et stochastiques pour la résolution numérique du problème de maintien de séparation entre aéronefs, Ph.D. dissertation, Institut Supérieur de l'Aéronautique et de l'Espace (ISAE), 2013.

[10] Gurobi Optimization, Inc., Gurobi optimizer reference manual, 2012. [Online]. Available: http://www.gurobi.com.

[11] T. Schouwenaars, Safe trajectory planning of autonomous vehicles, Ph.D. dissertation, Massachusetts Institute of Technology, Department of Aeronautics and Astronautics, Cambridge MA, 2006.

[12] J. Omer and J.-L. Farges, Hybridization of nonlinear and mixed-integer linear programming for aircraft separation with trajectory recovery, IEEE Transactions on Intelligent Transportation Systems, 14(3), 1218–1230, 2013.

[13] L. Pallottino, E. Feron, and A. Bicchi, Conflict resolution problems for air traffic management systems solved with mixed integer programming, IEEE Transactions on Intelligent Transportation Systems, 3, 3–11, 2002.

[14] A. Vela, S. Solak, J. Clarke, W. Singhose, E. Barnes, and E. Johnson, Near real-time fuel-optimal en route conflict resolution, IEEE Transactions on Intelligent Transportation Systems, 11, 826–837, 2010.

[15] A. Alonso-Ayuso, L. Escudero, and F. Martìn-Campo, Collision avoidance in air traffic management: A mixed-integer linear optimization approach, IEEE Transactions on Intelligent Transportation Systems, 12(1), 47–57, 2011.

[16] A. Vela, S. Solak, W. Singhose, and J.-P. Clarke, A mixed integer program for flight-level assignment and speed control for conflict resolution, in Proceedings of the 48th IEEE Conference on Decision and Control, 2009, pp. 5219–5226.

[17] A. Alonso-Ayuso, L. Escudero, P. Olaso, and C. Pizarro, Conflict avoidance: 0-1 linear models for conflict detection & resolution, TOP, 21, 485–504, 2013.

[18] D. Rey, C. Rapine, R. Fondacci, and N.-E. E. Faouzi, Potential air conflicts minimization through speed regulation, in TRB 91st Annual Meeting Compendium of Papers, 2012.

[19] S. Cafieri and N. Durand, Aircraft deconfliction with speed regulation: New models from mixed-integer optimization, Journal of Global Optimization, 58(4), 613–629, 2013.

[20] J. Omer, A space-discretized mixed integer linear model for solving air conflict with speed and heading maneuvers, 2014, Les Cahiers du GERAD G–2014–20, HEC Montréal, Canada.

[21] C. Frese and J. Beyerer, A comparison of motion planning algorithms for cooperative collision avoidance of multiple cognitive automobiles, in IEEE Intelligent Vehicles Symposium, 2011, Proceedings Paper, 1156–1162.

[22] R. A. Paielli, Modeling maneuver dynamics in air traffic conflict resolution, Journal of Guidance, Control, and Dynamics, 26, 407–415, 2003.

[23] SESAR Joint Undertaking, European ATM master plan, edition 2, Tech. Rep., 2012.

[24] A. Nuic, User manual for the Base of Aircraft Data (BADA), Eurocontrol, Tech. Rep. 11/03/08-08, 2011.